Exact Nonequilibrium Steady State of *XXZ* Circuits Boundary Driven with Arbitrary Resets or Fields

Vladislav Popkov[1,2] and Tomaž Prosen[1,3]
[1]*Department of Physics, Faculty of Mathematics and Physics, University of Ljubljana, Jadranska 19, SI-1000 Ljubljana, Slovenia*
[2]*Department of Physics, University of Wuppertal, Gaussstraße 20, 42119 Wuppertal, Germany*
[3]*Institute of Mathematics, Physics, and Mechanics, Jadranska 19, SI-1000 Ljubljana, Slovenia*

(Received 20 February 2025; accepted 11 July 2025; published 11 August 2025)

We propose a spatially inhomogeneous matrix product *Ansatz* for an exact many-body density operator of a boundary-driven *XXZ* quantum circuit. The *Ansatz* has formally infinite bond dimension and is fundamentally different from previous constructions. The circuit is driven by a pair of reset quantum channels applied on the boundary qubits, which polarize the qubits to arbitrary pure target states. Moreover, one of the reset channels can be replaced by an arbitrary local unitary gate, thus representing a hybrid case with coherent and incoherent driving. Analyzing the *Ansatz*, we obtain a family of relatively robust separable nonequilibrium steady states, which can be viewed as a circuit extension of spin-helix states and are particularly suited for experimental investigations.

DOI: 10.1103/31p7-lcgh

Introduction—The theory of open quantum systems [1–3] represents the backbone of quantum simulation engineering in the so-called noisy intermediate scale quantum (NISQ) era. Having exactly solvable models of strongly correlated (open) quantum systems, in particular, of the type of digital quantum circuits, is of unprecedented value for the control, benchmarking, and science demonstration purpose of NISQ devices (see, e.g., [4–7]).

An important paradigm in this context is that of integrable quantum spin chains driven out of equilibrium by dissipative processes at the chain's boundaries [8]. Most remarkably, it has been shown that the nonequilibrium steady state (NESS) of a Trotterized integrable *XXZ* quantum spin chain, realized as a brickwork quantum circuit, driven by a certain type of Kraus dissipator at the chain ends can be written as an infinite bond-dimension matrix product *Ansatz* (MPA) [9]. This protocol has later been simulated by a NISQ device [7]. The setup not only represents an elegant mathematical solution of a simple nontrivial correlated many-body model, but it also leads to interesting and sometimes exotic new physics, such as fractal transport coefficients (Drude weights) [10,11], insulating far-from-equilibrium spin transport, or negative differential conductance [12,13].

Recently, a new type of MPA with spatially inhomogeneous matrices has been introduced in order to solve the boundary-driven NESS of an XXZ/XYZ chain in the Zeno regime of asymptotically large boundary dissipation [14–16]. In this Letter, we report an unexpected extension of inhomogeneous infinite bond-dimension MPA for expressing a NESS of a brickwork *XXZ* circuit, driven by reset channels targeting arbitrary boundary states and/or external boundary magnetic field oriented in arbitrary direction. The auxiliary space has a tensor product structure of two replicas corresponding to "bra" and "ket" of the density matrix. However, unlike in all previous exactly solvable cases, the boundary reset-channel driving nontrivially couples these two replica spaces. In that sense, our *Ansatz* is fundamentally different from previous constructions, where the many-body density operator can be factorized in terms of a product (Cholesky-like decomposition [8]). Our results thus not only promise immediate applications in the context of NISQ simulators, but also hold the potential of extending the correlated two-replica MPA to other driven models. Moreover, we demonstrate an existence, for a specific set of boundary parameters, of a family of relatively robust (and separable) NESSs, which can be viewed as an extension to circuits of spin-helix states [17–21] that turned out to be prominent in cold-atom experiments [22,23].

Boundary reset-driven XXZ circuits—We consider a chain of $N+2$ qubits labeled by $0, 1, \ldots, N, N+1$. An *XXZ* gate, sometimes also referred to as a fSim gate [4,5], can be algebraically parametrized as

Published by the American Physical Society under the terms of the Creative Commons Attribution 4.0 International license. Further distribution of this work must maintain attribution to the author(s) and the published article's title, journal citation, and DOI.

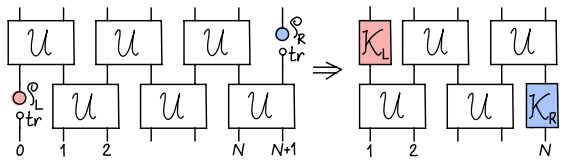


FIG. 1. 2-step reset driven XXZ circuit in folded notation. Empty circles represent a local traces while red and blue disks represent arbitrary pure boundary states. The right scheme correspond to an equivalent reduced circuit where squares represent boundary Kraus maps (details in text).

$$U=\begin{pmatrix}1&0&0&0\\0&a&b&0\\0&b&a&0\\0&0&0&1\end{pmatrix},\quad a\equiv\frac{q-q^{-1}}{q\lambda-(q\lambda)^{-1}},\quad b\equiv\frac{\lambda-\lambda^{-1}}{q\lambda-(q\lambda)^{-1}}. \tag{1}$$

U is unitary if (i) $|q|=1$ and $\lambda\in\mathbb{R}$ [easy plane regime (EPR)], or (ii) $q\in\mathbb{R}$ and $|\lambda|=1$ [easy axis regime (EAR)]. Note also $U^{-1}=U|_{q\to q^{-1}}=U|_{\lambda\to\lambda^{-1}}$, $\forall\ q,\lambda\in\mathbb{C}$. The gate acts on a pair of neighboring qubits via so-called folded map $\mathcal{U}:\mathrm{End}(\mathbb{C}^4)\to\mathrm{End}(\mathbb{C}^4)$ as $\mathcal{U}(\rho)=U\rho U^\dagger$. Assuming N to be odd (while similar construction can be given for N even also), we define a two-step dynamical protocol (see Fig. 1): In step 1, we apply a string of $(N+1)/2$ gates to all neighboring pairs of qubits $1,2,\ldots,N+1$ while qubit 0 is traced out and reset to an arbitrary pure state $\rho_{\mathrm{L}}=|\psi_{\mathrm{L}}\rangle\langle\psi_{\mathrm{L}}|$. In step 2, we similarly apply $(N+1)/2$ gates to qubits $0,\ldots,N$ and reset the last qubit to arbitrary pure state $\rho_{\mathrm{R}}=|\psi_{\mathrm{R}}\rangle\langle\psi_{\mathrm{R}}|$. This defines a simple many-body locally interacting (Trotterized XXZ) quantum channel, targeting specific local spin states at the ends. Here $\log|\lambda|$ represents the Trotter time step, so $\lambda\to1$ corresponds to continuous-time limit, governed by the paradigmatic XXZ spin chain [24–26]. However, we stress that our XXZ circuit is an interesting discrete-time dynamical system in its own right.

Ignoring the trivially separable state of the boundary qubit (left in step 1 and right in step 2), we can write an equivalent effective brickwork dynamical quantum channel acting on interior N qubits, labeled $1,2,\ldots,N$, as

$$\rho_{t+1}=\mathcal{M}(\rho_t),\qquad \mathcal{M}=\mathcal{M}_{\mathrm{o}}\mathcal{M}_{\mathrm{e}},$$
$$\mathcal{M}_{\mathrm{o}}=\mathcal{K}_{\mathrm{L}}\otimes\mathcal{U}^{\otimes(N-1)/2}\qquad \mathcal{M}_{\mathrm{e}}=\mathcal{U}^{\otimes(N-1)/2}\otimes\mathcal{K}_{\mathrm{R}}, \tag{2}$$

where $\mathcal{K}_{\mathrm{L/R}}:\mathrm{End}(\mathbb{C}^2)\to\mathrm{End}(\mathbb{C}^2)$ are the local boundary channels

$$\mathcal{K}_{\mathrm{L}}(\rho)=\mathrm{tr}_1U(\rho_{\mathrm{L}}\otimes\rho)U^\dagger,\quad \mathcal{K}_{\mathrm{R}}(\rho)=\mathrm{tr}_2U(\rho\otimes\rho_{\mathrm{R}})U^\dagger, \tag{3}$$

conveniently expressed in terms of pairs of Kraus matrices $\mathcal{K}_{\mathrm{L/R}}(\rho)=\sum_{\mu=1}^{2}K_{\mathrm{L/R}}^{[\mu]\dagger}\rho K_{\mathrm{L/R}}^{[\mu]}$,

$$K_{\mathrm{L}}^{[1]}=\frac{1}{\sqrt{1+|z|^2}}\begin{pmatrix}1&\frac{\lambda-\lambda^{-1}}{\lambda/q-q/\lambda}\bar z\\0&\frac{q-q^{-1}}{q/\lambda-\lambda/q}\end{pmatrix},$$
$$K_{\mathrm{L}}^{[2]}=\frac{1}{\sqrt{1+|z|^2}}\begin{pmatrix}\frac{q-q^{-1}}{q/\lambda-\lambda/q}\bar z&0\\\frac{\lambda-\lambda^{-1}}{\lambda/q-q/\lambda}&\bar z\end{pmatrix},$$
$$K_{\mathrm{R}}^{[1]}=\frac{1}{\sqrt{1+|w|^2}}\begin{pmatrix}1&\frac{\lambda-\lambda^{-1}}{\lambda/q-q/\lambda}\bar w\\0&\frac{q-q^{-1}}{q/\lambda-\lambda/q}\end{pmatrix},$$
$$K_{\mathrm{R}}^{[2]}=\frac{1}{\sqrt{1+|w|^2}}\begin{pmatrix}\frac{q-q^{-1}}{q/\lambda-\lambda/q}\bar w&0\\\frac{\lambda-\lambda^{-1}}{\lambda/q-q/\lambda}&\bar w\end{pmatrix}. \tag{4}$$

The boundary spinors are stereographically parametrized

$$|\psi_{\mathrm{L}}\rangle=\frac{1}{\sqrt{1+|z|^2}}\begin{pmatrix}1\\\bar z\end{pmatrix},\quad |\psi_{\mathrm{R}}\rangle=\frac{1}{\sqrt{1+|w|^2}}\begin{pmatrix}1\\\bar w\end{pmatrix}, \tag{5}$$

in terms of polar and azimuthal angles $z=\tan(\theta_{\mathrm{L}}/2)e^{i\phi_{\mathrm{L}}}$, $w=\tan(\theta_{\mathrm{R}}/2)e^{i\phi_{\mathrm{R}}}$. The goal of this Letter is to derive an elegant closed-form representation of a unique NESS density operator, i.e., fixed point of $\mathcal{M}$, Eq. (2): $\rho_\infty=\mathcal{M}(\rho_\infty)$.

Inhomogeneous Yang-Baxter equation—Let us denote physical space of N qubits as $\mathfrak{h}=(\mathbb{C}^2)^{\otimes N}$ and label local operators over $\mathfrak{h}$ which act nontrivially only on the n th tensor factor (qubit) by subscript n, e.g., Pauli operators $\sigma_n^{\mathrm{x,y,z}}$. In addition, we consider an infinite-dimensional auxiliary space $\mathfrak{a}$ spanned by basis vectors $\{|j\rangle_{\mathfrak{a}};j=0,1\ldots\}$. We now define a special type of inhomogeneous Lax operators and their conjugates, $L_{\mathfrak{a},n}^{\pm},L_{\mathfrak{a},n}^{\pm*}\in\mathrm{End}(\mathfrak{a}\otimes\mathfrak{h})$, which we construct as

$$L_{\mathfrak{a},n}^{+}=\sum_{j=0}^{\infty}\left[|j\rangle\langle j|_{\mathfrak{a}}A_n^{[n-2j]}D_n+|j\rangle\langle j+1|_{\mathfrak{a}}A_n^{[n-2j]}E_n\right],$$
$$L_{\mathfrak{a},n}^{-}=\sum_{j=0}^{\infty}\left[|j\rangle\langle j|_{\mathfrak{a}}E_nA_n^{[n-2j]}+|j\rangle\langle j+1|_{\mathfrak{a}}D_nA_n^{[n-2j]}\right],$$
$$L_{\mathfrak{a},n}^{+*}=\sum_{j=0}^{\infty}\left[|j\rangle\langle j|_{\mathfrak{a}}D_n^\dagger A_n^{[n-2j]\dagger}+|j\rangle\langle j+1|_{\mathfrak{a}}E_n^\dagger A_n^{[n-2j]\dagger}\right],$$
$$L_{\mathfrak{a},n}^{-*}=\sum_{j=0}^{\infty}\left[|j\rangle\langle j|_{\mathfrak{a}}A_n^{[n-2j]\dagger}E_n^\dagger+|j\rangle\langle j+1|_{\mathfrak{a}}A_n^{[n-2j]\dagger}D_n^\dagger\right], \tag{6}$$

where

$$A^{[n]}=\begin{pmatrix}1&-q^{-n}/z\\q^nz&-1\end{pmatrix}=\begin{pmatrix}1\\q^nz\end{pmatrix}(1,-q^{-n}/z),$$
$$D=\begin{pmatrix}\lambda&0\\0&1\end{pmatrix},\qquad E=\begin{pmatrix}1&0\\0&\lambda\end{pmatrix}. \tag{7}$$

Note that $z \in \mathbb{C}$ is a free formal parameter here. Interpreting the gate $U_{n,n+1}$ as a braid-type R matrix of the unitary six-vertex model, we postulate the following inhomogeneous (i.e., explicitly n-dependent) Yang-Baxter identities (or RLL relations):

$$U_{n,n+1}L^{+}_{\mathfrak{a},n}L^{-}_{\mathfrak{a},n+1} = L^{-}_{\mathfrak{a},n}L^{+}_{\mathfrak{a},n+1}U_{n,n+1},$$
$$U_{n,n+1}L^{+*}_{\mathfrak{a},n}L^{-*}_{\mathfrak{a},n+1} = L^{-*}_{\mathfrak{a},n}L^{+*}_{\mathfrak{a},n+1}U_{n,n+1}. \tag{8}$$

The identities (8) are brickwork analogs of the local divergence condition [15,16] for the XXZ Hamiltonian and reduce to the latter in the limit $\lambda \to 1$. For proving these identities, and noting that a shift $j \to j+1$ in auxiliary space is equivalent to $z \to q^2 z$, it is enough to establish that they hold for matrix elements, $\langle 0|\bullet|0\rangle_{\mathfrak{a}}$, $\langle 0|\bullet|1\rangle_{\mathfrak{a}}$, $\langle 0|\bullet|2\rangle_{\mathfrak{a}}$, which is straightforward.

Explicit inhomogeneous matrix product NESS—Let us now define the so-called doubled Lax operators acting over tow-replica auxiliary space, $\mathbb{L}^{\pm}_{\mathfrak{ab},n} \in \mathrm{End}(\mathfrak{a} \otimes \mathfrak{b} \otimes \mathfrak{h})$, $\mathfrak{b} \simeq \mathfrak{a}$, as $\mathbb{L}^{\pm}_{\mathfrak{ab},n} = L^{\pm}_{\mathfrak{a},n}L^{\pm *}_{\mathfrak{b},n}$ again satisfying RLL identity,

$$U_{n,n+1}\mathbb{L}^{+}_{\mathfrak{ab},n}\mathbb{L}^{-}_{\mathfrak{ab},n+1}U^{\dagger}_{n,n+1} = \mathbb{L}^{-}_{\mathfrak{ab},n}\mathbb{L}^{+}_{\mathfrak{ab},n+1}. \tag{9}$$

The NESS fixed point can be conveniently split into even-odd two-cycle,

$$\rho'_{\infty} = \mathcal{M}_{\mathrm{e}}(\rho_{\infty}), \qquad \rho_{\infty} = \mathcal{M}_{\mathrm{o}}(\rho'_{\infty}), \tag{10}$$

for which we postulate the matrix product *Ansätze*,

$$\rho_{\infty} = \langle \mathrm{L}|\mathbb{L}^{+}_{\mathfrak{ab},1}\mathbb{L}^{-}_{\mathfrak{ab},2}\mathbb{L}^{+}_{\mathfrak{ab},3}\cdots\mathbb{L}^{-}_{\mathfrak{ab},N-1}\mathbb{L}^{+}_{\mathfrak{ab},N}|\mathrm{R}\rangle,$$
$$\rho'_{\infty} = \langle \mathrm{L}|\mathbb{L}^{-}_{\mathfrak{ab},1}\mathbb{L}^{+}_{\mathfrak{ab},2}\mathbb{L}^{-}_{\mathfrak{ab},3}\cdots\mathbb{L}^{+}_{\mathfrak{ab},N-1}\mathbb{L}^{-}_{\mathfrak{ab},N}|\mathrm{R}\rangle, \tag{11}$$

where

$$\langle \mathrm{L}| = \sum_{j,j'} \ell_{j,j'}\langle j|_{\mathfrak{a}}\langle j'|_{\mathfrak{b}}, \quad |\mathrm{R}\rangle = \sum_{j,j'} r_{j,j'}|j\rangle_{\mathfrak{a}}|j'\rangle_{\mathfrak{b}} \tag{12}$$

are the boundary vectors as elements of two-replica auxiliary space. $\langle \mathrm{L}|$ and $|\mathrm{R}\rangle$ can also be interpreted as auxiliary density matrices. For instance, Hermiticity of $\rho_{\infty}, \rho'_{\infty}$ is implied by $\ell_{j,j'} = \overline{\ell}_{j',j}$, $r_{j,j'} = \bar{r}_{j',j}$. Fixed-point conditions (10) trivially follow by telescoping the bulk relation (9), if the additional boundary equations are satisfied,

$$\langle \mathrm{L}|\left(\mathbb{L}^{+}_{\mathfrak{ab},1} - \sum_{\mu} K^{[\mu]\dagger}_{\mathrm{L},1}\mathbb{L}^{-}_{\mathfrak{ab},1}K^{[\mu]}_{\mathrm{L},1}\right) = 0, \tag{13}$$

$$\left(\mathbb{L}^{-}_{\mathfrak{ab},N} - \sum_{\mu} K^{[\mu]\dagger}_{\mathrm{R},N}\mathbb{L}^{+}_{\mathfrak{ab},N}K^{[\mu]}_{\mathrm{R},N}\right)|\mathrm{R}\rangle = 0. \tag{14}$$

For example, the left and right boundary equations (13) and (14) should fix $\ell_{j,j'}$ and $r_{j,j'}$, respectively. We assume that an exact solution should exist within a truncated auxiliary space considering only J_{L} states $\{|j\rangle_{\mathfrak{a},\mathfrak{b}}; j = 0,1,\ldots,J_{\mathrm{L}}-1\}$ at the left boundary. Because of band triangular structure of Lax operators (6), one has to consider $J_n = J_{\mathrm{L}} + n$ auxiliary states at site n and finally $J_{\mathrm{R}} = J_{\mathrm{L}} + N$ states at the right boundary.

Easy plane regime—In order to proceed toward explicit solutions of the above equations, we have to specify the magnetic regime of the unitary six-vertex model (1). We start with the EPR, $|q| = 1$ and $\lambda \in \mathbb{R}$, implying

$$A^{[n]\dagger} = \begin{pmatrix} 1 & q^{-n}\bar{z} \\ -q^{n}/\bar{z} & -1 \end{pmatrix}, \qquad D^{\dagger} = D, \qquad E^{\dagger} = E.$$

We find explicit solution of the left boundary equation (13) for $J_{\mathrm{L}} = 2$, exactly when z equals the polarization of the left target state in (5), unique up to a scale

$$\ell_{0,0} = \frac{\lambda+\lambda^{-1}}{2} + \frac{\lambda-\lambda^{-1}}{2}\frac{|z|^2-1}{|z|^2+1}, \qquad \ell_{0,1} = \ell_{1,0} = 1,$$
$$\ell_{1,1} = \frac{\lambda+\lambda^{-1}}{2} - \frac{\lambda-\lambda^{-1}}{2}\frac{|z|^2-1}{|z|^2+1}. \tag{15}$$

The right boundary equation (14) then amounts to linear recursion relations for $r_{j,j'}$, which we can solve in the closed form, again uniquely up to overall factor

$$r_{j,j'} = c_{j,j'}\prod_{k=0}^{j-1} b_{k-M}\prod_{k=0}^{j'-1}\bar{b}_{k-M}, \quad b_n = \frac{\lambda z q^{-n} - w q^{n}}{z q^{-n-1} - \lambda w q^{n+1}}, \tag{16}$$

where $j, j' = 0,1,\ldots,N+1$, $M = (N+1)/2$ is an integer, and

$$c_{j,j'} = (-1)^{j-j'}\left(|z|q^{j'-j} + |z|^{-1}q^{j-j'}\right). \tag{17}$$

Note that both left and right boundary vectors are generally nonseparable with respect to partitioning of a pair of auxiliary spaces $\mathfrak{a} \otimes \mathfrak{b}$. In fact, the Schmidt rank for both boundary vectors is equal to 2 [for the right boundary this follows from the presence of two terms in expression (17)]. Thus, (11) cannot be factorized into a product of two Cholesky-type factors as was the case in all the previous solvable instances [8,14–16]. The key properties of the model that lead to nonseparability are finite Trotter time step $\log\lambda \neq 0$ and reset channels breaking U(1) symmetry, i.e., $z, w \neq 0, \infty$ in (5). As the Trotter parameter approaches zero ($\lambda \to 1$), both boundary vectors (15) and (16) become factorizable.

Easy axis regime—In EAR, $q \in \mathbb{R}$ and $|\lambda| = 1$, we have the following conjugated matrices:

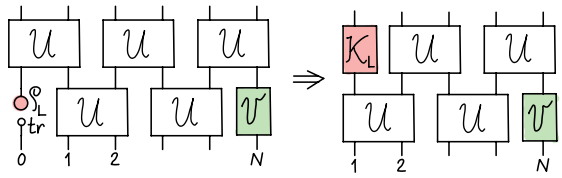


FIG. 2. Hybrid-driven XXZ circuit in folded notation where the left boundary is driven by the reset channel and the right boundary by the local unitary gate. Note that the total number of physical qubits $(N+1)$ is now one less than in the two-reset setup in Fig. 1.

$$A^{[n]\dagger}=\begin{pmatrix}1 & q^n\bar{z}\\ -q^{-n}/\bar{z} & -1\end{pmatrix},\quad D^\dagger=E/\lambda,\quad E^\dagger=D/\lambda,$$

entering the construction of double Lax operators $\mathbb{L}^{\pm}_{\mathfrak{ab},n}$. Following analogous steps as for EPR we again find an explicit nonseparable solution for $J_{\rm L}=2$, namely,

$$\ell_{0,0}=\ell_{1,1}=1\qquad \ell_{0,1}=\overline{\ell}_{1,0}=\frac{\lambda|z|+\lambda^{-1}|z|^{-1}}{|z|+|z|^{-1}},\tag{18}$$

and the right boundary vector given by exactly the same expression (16) but $c_{j,j'}$ modified to

$$c_{j,j'}=(-1)^{j+j'}\left(|z|q^{2M-j-j'}+|z|^{-1}q^{j+j'-2M}\right).\tag{19}$$

Hybrid (coherent-incoherent) boundary driving—Here we show that a similar structure of NESS exists for a hybrid boundary-driven setup with the reset channel $\mathcal{K}_{\rm L}$, Eq. (3) on the left, while the right end qubit $n=N$ is driven by an arbitrary local unitary channel (Fig. 2)

$$\mathcal{V}(\rho)=V\rho V^\dagger,\quad V=\frac{1}{\sqrt{1+t^2}}\begin{pmatrix}(uv)^{-1} & -u^{-1}vt\\ uv^{-1}t & uv\end{pmatrix},\tag{20}$$

where $u=e^{i\alpha}$, $v=e^{i\gamma}$, $t=\tan\beta$, with $\alpha,\beta,\gamma\in\mathbb{R}$ being the standard Euler angles. We postulate that the NESS fixed point of this problem is given by the same *Ansatz* (11). The left boundary equation (13) holds, so we retrieve the same solution for the left boundary vector (15) or (18), in the EPR or EAR, respectively. The right boundary equation (14), however, needs to be replaced by

$$\left(\mathbb{L}^{-}_{\mathfrak{ab},N}-V_N\mathbb{L}^{+}_{\mathfrak{ab},N}V_N^\dagger\right)|\mathrm{R}\rangle=0.\tag{21}$$

Remarkably, the solution of the recurrence scheme for $r_{j,j'}$ following from (21) is now identical in both regimes (EPR and EAR) and reads

$$r_{j,j'}=(-1)^{j-j'}\prod_{k=0}^{j-1}g_{k-M}\prod_{k=0}^{j'-1}\bar{g}_{k-M},$$
$$g_n=\frac{(1-v^2ztq^{-2n-1})z\lambda-u^2(tq^{2n+1}+v^2z)}{(1-v^2ztq^{-2n-1})z-u^2(tq^{2n+1}+v^2z)\lambda},\tag{22}$$

where $j,j'=0,1,\ldots,N+1$ and $M=(N+1)/2$. Note that the product (separable) form of the boundary vector (22) is a consequence of unitarity of the right boundary channel. This solution partly generalizes a related setup in the continuous-time Lindbladian case and transverse field [27].

Spin helices in brickwork circuits—Simple analysis of zeros and poles of the coefficients b_n in (16) leads to prediction of remarkably simple pure and separable NESS: A specific choice of the right boundary reset

$$w=q^{N+1}z\lambda,\tag{23}$$

corresponding to $b_{-M}=0$, leads to $r_{i,j}=\delta_{i,0}\delta_{j,0}$ and to separable NESS, $\rho_\infty=|\Psi_S^+\rangle\langle\Psi_S^+|$, $\rho'_\infty=|\Psi_S^-\rangle\langle\Psi_S^-|$,

$$|\Psi_S^\pm\rangle=|\psi_1^\pm\rangle\otimes|\psi_2^\mp\rangle\otimes|\psi_3^\pm\rangle\otimes|\psi_4^\mp\rangle\cdots|\psi_N^\pm\rangle,\tag{24}$$

$$|\psi_n^+\rangle=\begin{pmatrix}1\\ zq^n\end{pmatrix},\qquad |\psi_n^-\rangle=\begin{pmatrix}1\\ \lambda zq^n\end{pmatrix}.\tag{25}$$

In EPR the arrangement of qubits in the state (24) represents a distorted helix with wavelength $\Lambda=(2\pi i)/(\log q)$: the azimuthal angle of the helix $\varphi(n)=\eta n$, $\eta=-i\log q$ grows linearly with the position n, while the polar angle exhibits even-odd staggering with values θ_L, θ_R, where $\tan(\theta_R/2)=\lambda\tan(\theta_L/2)$. A schematic picture of the EPR helix is shown in Fig. 3. In the continuous-time limit, $\lambda\to1$, the state (24) becomes a perfect spin helix. With some abuse of notations, we shall refer to (24) as a "brickwork helix" or just "helix" state. Like their continuous-time counterparts, brickwork helices are very atypical chiral states with nonzero size-independent spin current. In EAR, q in (24) is real and λ is unimodular. Correspondingly, the EAR counterpart of the helix, Fig. 3, does not form a spiral, but for large N the qubit polarization along the chain approaches either the state $\uparrow\equiv\binom{1}{0}$ or

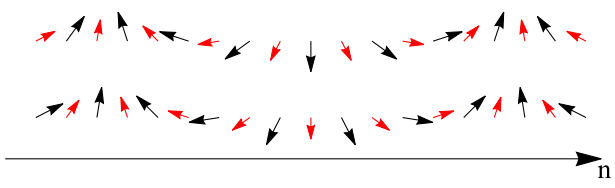


FIG. 3. Top view (XY-plane projection) of the spin polarizations in the EPR brickwork helix (24) with $z=1$, $\lambda=\tan(\pi/8)$, and $\eta=3\pi/20$. Lower and upper arrangements correspond to even and odd steps of the evolution, see (11).

$\downarrow \equiv \binom{0}{1}$, depending on whether $|q| < 1$ or $|q| > 1$. In addition, there is a staggering (25), i.e., even and odd site polarizations have different azimuthal angles.

Analogously, a pole in b_{N-M} ($1/b_{N-M} = 0$) yields a helix with inverted helicity, namely, a choice

$$z = w\lambda q^{N+1} \tag{26}$$

yields again a pure NESS, of exactly the same form as (24) with redefinitions $|\psi_n^+\rangle = \binom{1}{zq^{-n}}$, $|\psi_n^-\rangle = \binom{\lambda}{zq^{-n}}$.

Significance of the distorted spin helix (24) and its counterpart with opposite helicity for the circuit (Fig. 1) lies beyond just being exact NESS for the special choice of the right boundary conditions (23) or (26). It lies in its robustness: indeed, due to the Yang-Baxter relation (9), the helix is reproduced locally in the bulk after every cycle. Correspondingly, regardless of conditions imposed on the right boundary, the helix after one cycle will only be changed at the two rightmost sites, while everywhere else it will stay intact. It requires a time of order of system size N to destroy the helix completely, while a typical state will be destroyed after one time step. Being thus exceptionally robust, and in addition, easily creatable (being a factorized state), the helix can be used for calibration purposes, similar to its facility in the continuous-time counterpart $\lambda \to 0$ in cold atoms [22].

A slight modification of condition (23),

$$w = q^{N+1-2m_k} z\lambda, \tag{27}$$

with integer $m_k = 1, 2, \ldots$ leads to cropping of the right boundary vector to dimension $(m_k + 1)^2$, $r_{j,j'} = 0$ if $j > m_k$ or $j' > m_k$. The respective NESS is a mixed state of reduced rank, e.g., $\mathrm{rank(NESS)} = 1, N+1, \binom{N+1}{2} + 1$ for $m_k = 0$, 1, 2 and can be viewed as consisting from imperfect helices with m_k kinks (in analogy to [21]). For helices with inverted helicity, the analog of (27) reads $z/w = \lambda q^{N+1-2m_k}$, generalizing (26).

In the End Matter, we discuss simple observables for detection of helix states.

Discussion—We have presented an exact solution for the nonequilibrium steady state of brickwork circuits in two cases: (i) with two reset channels at the boundaries and (ii) one reset channel at one boundary and local field at another boundary. The system we considered can be directly realized experimentally, with technique belonging to the experimental toolbox [5,6]. We also identified the simplest yet nontrivial steady states of the driven brickwork circuits, brickwork helices (24), which should be of direct experimental relevance being especially robust and easily manipulatable: these states feature qubits, arranged as helices with even-odd site staggering. The period of the helix, $\Lambda = 2\pi i/\log[q]$, fixed by the anisotropy parameter q of the principal bulk gate (1), is system size independent. Brickwork helices and their descendants, helices with kinks (27), are identifiable by measuring just a one-point correlation in the steady state as exemplified in Fig. 4, which again can be of direct relevance for an experiment.

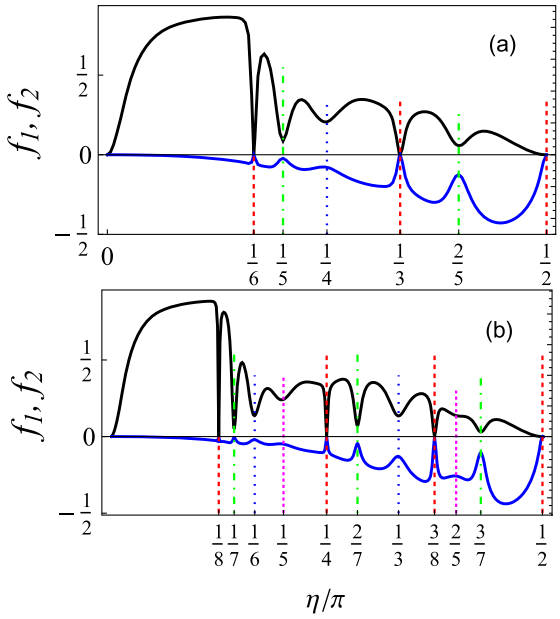


FIG. 4. Helix indicators: f_1 (A1) (upper black curve), f_2 (A2) (lower blue curve) measured in the NESS, in the easy plane regime, versus the XXZ anisotropy η/π, for system of $N = 11$ (a) and $N = 15$ (b) sites. Parameters: $z = 1, \lambda = \exp[0.9], w = z\lambda$. Zeros of the observable coincide with the pure helix condition $(N+1)\eta = 0 \pmod{2\pi}$, (red dashed lines), where the NESS looks as in Fig. 3, with the lattice period $T = 2\pi/\eta$. Other less pronounced minima occur at the anisotropy values leading to a helix with integer number of kinks $(N + 1 - 2m_k)\eta = 0 \pmod{2\pi}$, $m_k = 1$, 2, 3 (green, blue, and magenta dashed lines, respectively).

The technical framework introduced here should be directly applicable to other reset-driven brickwork circuits with local gates satisfying the (braid) Yang-Baxter equation. In this regard, we are inclined to see the nontrivial coupling between the auxiliary spaces as a necessary resource to find further integrable dissipatively driven quantum circuits. Moreover, based on preliminary numerical evidence from studying complex spacing ratios [28] of the spectrum of superoperator $\mathcal{M}$ (2), we conjecture full integrability of our boundary reset discrete-time Liouvillian (2), contrary to previous solvable NESS boundary settings [29].

Acknowledgments—V. P. and T. P. acknowledge support by ERC Advanced Grant No. 101096208—QUEST, and Research Programme P1-0402 of Slovenian Research and Innovation Agency (ARIS). V. P. is also supported by Deutsche Forschungsgemeinschaft through DFG Project No. KL645/20-2.

Data availability—No data were created or analyzed in this study.

[1] H.-P. Breuer and F. Petruccione, *The Theory of Open Quantum Systems* (Oxford University Press, New York, 2002).

[2] M. A. Nielsen and I. L. Chuang, *Quantum Computation and Quantum Information* (Cambridge University Press, Cambridge, England, 2010).

[3] C. Gardiner and P. Zoller, *Quantum Noise: A Handbook of Markovian and Non-Markovian Quantum Stochastic Methods with Applications to Quantum Optics* (Springer Science & Business Media, New York, 2004).

[4] B. Foxen, C. Neill *et al.*, Demonstrating a continuous set of two-qubit gates for near-term quantum algorithms, Phys. Rev. Lett. **125**, 120504 (2020).

[5] A. Morvan, T. Andersen *et al.*, Formation of robust bound states of interacting microwave photons, Nature (London) **612**, 240 (2022).

[6] X. Mi, A. Michailidis *et al.*, Stable quantum-correlated many-body states through engineered dissipation, Science **383**, 1332 (2024).

[7] E. Rosenberg, T. Andersen *et al.*, Dynamics of magnetization at infinite temperature in a Heisenberg spin chain, Science **384**, 48 (2024).

[8] T. Prosen, Matrix product solutions of boundary driven quantum chains, J. Phys. A **48**, 373001 (2015).

[9] M. Vanicat, L. Zadnik, and T. Prosen, Integrable trotterization: Local conservation laws and boundary driving, Phys. Rev. Lett. **121**, 030606 (2018).

[10] T. Prosen, Open *xxz* spin chain: Nonequilibrium steady state and a strict bound on ballistic transport, Phys. Rev. Lett. **106**, 217206 (2011).

[11] M. Ljubotina, L. Zadnik, and T. Prosen, Ballistic spin transport in a periodically driven integrable quantum system, Phys. Rev. Lett. **122**, 150605 (2019).

[12] G. Benenti, G. Casati, T. Prosen, D. Rossini, and M. Žnidarič, Charge and spin transport in strongly correlated one-dimensional quantum systems driven far from equilibrium, Phys. Rev. B **80**, 035110 (2009).

[13] T. Prosen, Exact nonequilibrium steady state of a strongly driven open *xxz* chain, Phys. Rev. Lett. **107**, 137201 (2011).

[14] V. Popkov, T. Prosen, and L. Zadnik, Exact nonequilibrium steady state of open *xxz*/*xyz* spin-1/2 chain with dirichlet boundary conditions, Phys. Rev. Lett. **124**, 160403 (2020).

[15] V. Popkov, T. Prosen, and L. Zadnik, Inhomogeneous matrix product ansatz and exact steady states of boundary-driven spin chains at large dissipation, Phys. Rev. E **101**, 042122 (2020).

[16] V. Popkov, X. Zhang, and T. Prosen, Boundary-driven xyz chain: Inhomogeneous triangular matrix product ansatz, Phys. Rev. B **105**, L220302 (2022).

[17] V. Popkov, J. Schmidt, and C. Presilla, Spin-helix states in the xxz spin chain with strong boundary dissipation, J. Phys. A **50**, 435302 (2017).

[18] S. Kühn, F. Gerken, L. Funcke, T. Hartung, P. Stornati, K. Jansen, and T. Posske, Quantum spin helices more stable than the ground state: Onset of helical protection, Phys. Rev. B **107**, 214422 (2023).

[19] A. Tripathi, F. Gerken, P. Schmitteckert, M. Thorwart, M. Trif, and T. Posske, Generalized Josephson effect with arbitrary periodicity in quantum magnets, Phys. Rev. Res. **7**, 013272 (2025).

[20] E. S. Ma, K. L. Zhang, and Z. Song, Steady helix states in a resonant *XXZ* Heisenberg model with Dzyaloshinskii-Moriya interaction, Phys. Rev. B **106**, 245122 (2022).

[21] X. Zhang, A. Klümper, and V. Popkov, Phantom Bethe roots in the integrable open spin-$\frac{1}{2}$ *XXZ* chain, Phys. Rev. B **103**, 115435 (2021).

[22] P. N. Jepsen, Y. K. â. Lee, H. Lin, I. Dimitrova, Y. Margalit, W. W. Ho, and W. Ketterle, Long-lived phantom helix states in Heisenberg quantum magnets, Nat. Phys. **18**, 899 (2022).

[23] P. N. Jepsen, W. W. Ho, J. Amato-Grill, I. Dimitrova, E. Demler, and W. Ketterle, Transverse spin dynamics in the anisotropic Heisenberg model realized with ultracold atoms, Phys. Rev. X **11**, 041054 (2021).

[24] E. Lieb and F. Y. Wu, *Two Dimensional Ferroelectric Models, in Phase Transitions and Critical Phenomena* (Academic Press, London, 1972).

[25] R. J. Baxter, *Exactly Solved Models in Statistical Mechanics* (Academic Press, New York, 1982).

[26] V. E. Korepin, N. M. Bogolyubov, and A. G. Izergin, *Quantum Inverse Scattering Method and Correlation Functions* (Cambridge University Press, Cambridge, England, 1993).

[27] M. Yao, A. Lingenfelter, R. Belyansky, D. Roberts, and A. A. Clerk, Hidden time reversal in driven *xxz* spin chains: Exact solutions and new dissipative phase transitions, Phys. Rev. Lett. **134**, 130404 (2025).

[28] L. Sá, P. Ribeiro, and T. Prosen, Complex spacing ratios: A signature of dissipative quantum chaos, Phys. Rev. X **10**, 021019 (2020).

[29] G. Akemann, M. Kieburg, A. Mielke, and T. Prosen, Universal signature from integrability to chaos in dissipative open quantum systems, Phys. Rev. Lett. **123**, 254101 (2019).

End Matter

Appendix—To detect the helix states, instead of measuring the NESS magnetization current, which is a complicated four-point correlation for a brickwork *XXZ* circuit, see [11], we propose to measure a simple one-point correlation, $\langle\sigma_1^+\rangle = \mathrm{tr}(\sigma_1^+\rho_\infty)$, which turns out to be extremely sensitive to the presence of helices, and their descendants (helices with kinks). From complex $\langle\sigma_1^+\rangle$, we construct two scalar helix indicators

$$f_1 = 1 - \frac{\arg(\langle\sigma_1^+\rangle/z)}{\eta}, \tag{A1}$$

$$f_2 = -1 + |(|z| + |z|^{-1})\langle\sigma_1^+\rangle|, \tag{A2}$$

f_1 relating to the twisting angle between the first qubit and the left reset state, and f_2 relating to purity of the first qubit. Both indicators vanish $f_1 = f_2 = 0$ for the perfect brickwork helix (24).

According to (23) and (26), we expect the helix (24) to appear at fine-tuned values of anisotropy $\eta = -i \log q$ provided that the boundary reset states satisfy

$$|w/z| = \lambda \quad \text{or} \quad |w/z| = 1/\lambda. \tag{A3}$$

In Fig. 4, we plot f_1 and f_2 versus the anisotropy η in a chain with reset channels fulfilling (A3). Apart from the expected zeros of f_1, f_2 signalizing pure NESS, we find sharp local minima of f_1 and $-f_2$, exactly at the η values (27) where we predicted helix descendants to occur. The number of pure helices and their descendants increase linearly with the system size N and, in addition, for larger N more and more descendants are resolved in $f_1(\eta), f_2(\eta)$ dependence. This can be seen by comparing the upper and lower panels of Fig. 4. Indeed for $N = 11$ one easily identifies minima corresponding to $m_{\mathrm{k}} = 0, 1, 2$ in (27), while for $N = 15$ one can also recognize the minima corresponding to states with three kinks $m_{\mathrm{k}} = 3$. In absence of the resonant condition (A3), the resonance peaks smear out and the local chirality of the NESS $(1 - f_1)$ decreases with system size N irrespective of the anisotropy (data not shown).

Hybrid systems (Fig. 2) exhibit similar phenomenology and even larger sensitivity to the presence of helices.